The Role of $Ca_v1.3$ Channels in Cardiac Pacemaking: Developing a Single-Cell Rabbit 3D Model

Eugenio Ricci[1], Chiara Bartolucci[1], Eleonora Torre[2], Pietro Mesirca[2], Matteo E Mangoni[2], Stefano Severi[1]

[1]University of Bologna, Italy
[2]Institut de Génomique Fonctionnelle, Université de Montpellier, CNRS, Montpellier, France

Abstract

Robust electrophysiological and functional evidence shows the importance of L-type $Ca_v1.3$ channels in sinoatrial node pacemaker activity. However, little is still known about its quantitative contribution in rabbit sinoatrial node cells. Therefore, we developed 0D and 3D computational models of single rabbit sinoatrial node myocytes, starting from previously validated "membrane" and "calcium-clock" models of cardiac pacemaking. A formulation for $I_{Ca_v1.3}$ gained from mouse sinoatrial myocytes was included, while the $Ca_v1.2$ current was modified so that the sum of the $Ca_v1.2$ ($I_{Ca_v1.2}$) and $Ca_v1.3$ ($I_{Ca_v1.3}$) components would reproduce the original I_{CaL} I/V relationship. Additionally, key ion channels (e.g. $Ca_v1.3$, $Ca_v1.2$, NCX) were spatially co-localized with Ryanodine receptors in different amounts. Numerical simulations show that the mathematical models reproduce basal pacemaker activity, main Action Potential features and cell-wide Calcium Transient features. Further validation was performed against available experimental data on ion channel blocks and autonomic nervous stimulation. In conclusion, we show the relevance of $Ca_v1.3$ channels contribution to rabbit sinoatrial activity using a computational model that will allow further highly detailed investigation of pacemaking mechanisms.

1. Introduction

$Ca_v1.3$ channels show more hyperpolarized half activation voltage and faster activation kinetics compared to cardiac excitation-contraction coupling $Ca_v1.2$ isoform. This allows the $Ca_v1.3$-dependent current ($I_{Ca_v1.3}$) to supply inward current during the diastolic depolarization phase, suggesting the importance of these channels in cardiac pacemaking regulation. Indeed, genetic ablation or pharmacologic inhibition of $Ca_v1.3$ in mice severely reduce pacemaker activity [1, 2], while loss of function in $Ca_v1.3$ channels leads to congenital sinoatrial dysfunction in humans. In mice, $Ca_v1.3$ channels were shown to synchronize RyR release [2], thus controlling the calcium-clock activity. However, due to the absence of a selective blocker, no data on larger mammals, such as rabbits, is available yet. In this work, we aim at providing quantitative information on the role of $Ca_v1.3$ channels in the generation and regulation of pacemaking by developing detailed, 3-dimensional mathematical model of a rabbit single sinoatrial node cell.

2. Methods

The model features detailed descriptions of 1) Calcium Release Units (CRUs) organization from Maltsev and colleagues [3] and 2) membrane current formulations from the Severi-DiFrancesco (SDiF) model [4].

2.1. Structure

The cell is represented as a cylinder divided in three different layers: the subcellular space, with 180x444 voxels of 120x120 nm of size, a middle layer with 60x148 voxels of 360x360 nm (thus, with a 9:1 surface ratio with the subspace) and a single central core compartment. Calcium diffusion between the voxels is modeled with the following reaction-diffusion equation, solved with first-order finite differences:

$$\frac{\partial Ca_{sub}}{\partial t} = D\nabla^2 Ca_{sub} - \Sigma J \tag{1}$$

555 CRUs, formed by clusters of 12x12 RyR channels that can open stochastically, are randomly distributed along the cell surface.

2.2. I_{Ca_v13} Formulation

The novel part of this work consists in the inclusion of the mice $I_{Ca_v1.3}$ formulation by Mangoni and colleagues [1, 5] for the steady-state curves. A minor shift of the

activation curve to the right (+1 mV) and a reduction in the slope factor (from 6.3 to 4) were applied to reproduce rabbit action potential (AP) biomarkers (Table 1). Furthermore, the kinetics adopted for $I_{Ca_v1.3}$ current were borrowed from the original I_{CaL} current of the SDiF model [4], with the voltage-dependent activation time constants scaled by a factor 0.9. The inactivation time constants were reduced to 40% of the original value for both Ca_{v13} and Ca_{v12} isoforms. In addition, a Goldman-Hodgkin-Katz formulation for the driving force was employed for Ca_{v13}, instead of the linear one from mouse [1]. The ratio between Ca_{v13} and Ca_{v12} maximal permeabilities was equal to 2.91, as in mice [1, 5]. However, to achieve an IV curve peak at positive voltages (+10 mV) for $I_{Ca_v1.2}$, as seen in mice experiments [1], both its steady state activation and inactivation curves were shifted +25 mV to the right and the slope factor was increased from 4 to 5. Fig. 1 shows the IV curves of the total I_{CaL} current, computed as the sum of the $Ca_v1.3$ and $Ca_v1.2$ components.

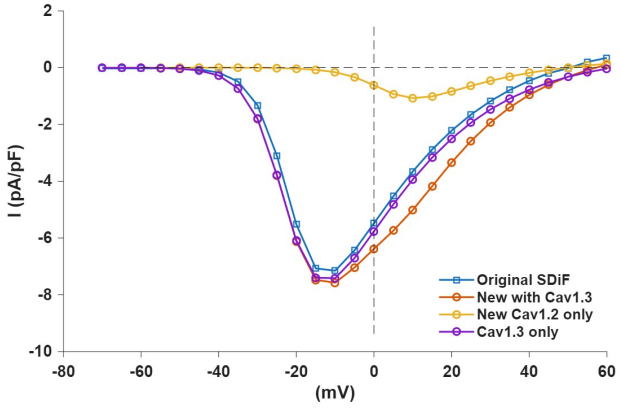

Figure 1. Comparison of I/V curves for total I_{CaL} current of the original SDiF and of the present formulations. The latter is computed as the sum of the $Ca_v1.3$ and $Ca_v1.2$ components.

2.3. Channel Co-localization

Since data on co-localization of $Ca_v1.3$, $Ca_v1.2$, and NCX channels with CRUs are not available for rabbit SAN cells, a sensitivity analysis was performed by varying the distribution of fluxes for these 3 channels. For example, when Ca_v channels were considered completely co-localized with CRUs, this meant that 100% of Ca^{2+} influx was distributed to the volume (equal to 9 subspace voxels) abutting each of the 555 CRUs of the model and that 2) the channels sensed the local (i.e. of each CRU) Ca^{2+} concentrations. Differently, when only a portion of channels were co-localized with CRUs, the other channels provided Ca^{2+} flux to the remaining part of the subcellular space (the one not occupied by CRUs). Accordingly, these channels were calcium-dependently inactivated by the average global Ca^{2+} outside of the CRUs. To deal with the higher local Ca^{2+} concentrations, the channel sensitivity to calcium-depedent inactivation had to be lowered by increasing the Km_{fCa} parameter of the Hill curve by a factor 10. Three different levels of co-localization were tested for NCX (0, 25, 50%) and Ca_{v13} (60, 80 and 100%) while Ca_{v12} channels co-localization was varied in the [20, 100]% range with 20% increments. A cost function was defined as in [6] to assess the parameter combination that provided the best reproduction of experimental AP biomarkers and cellular responses to stimulation (explained below). In this way, the "best fitting" model was obtained and used for further simulations. Finally, small-conductance, Ca^{2+}-activated potassium channels, modeled according to a recent formulation [7], were 100% co-localized with CRUs.

2.4. 0D Implementation

A 0-dimensional, common-pool version of the single rabbit SAN cell model was obtained by modifying the L-type calcium current as done for the 3D version, starting from the original SDiF model. The slope factor of the steady-state activation curve (4.5) and the voltage-dependent time constants of the Ca_{v13} isoform (multiplied by 0.9 and 0.75 respectively for activation and inactivation) were again tuned to better reproduce experimental AP biomarkers (Table 1).

All simulations were run in Matlab R2019b for 300 s (in 0D) and 15 s (in 3D, which took roughly 20 hours on a standard desktop pc). Simulations with administration of 1 µM isoproterenol (ISO), 10 nM acetylcholine (ACh), 3 µM ivabradine (Iva) or ion channel blocks started from 15 s control conditions. Action potential biomarkers were computed as in our previous works [8].

3. Results

The sensitivity analysis showed that the model obtaining the lowest cost was the one with 100% $Ca_v1.3$, 20% $Ca_v1.2$ and 0%NCX colocalization. As reported in Table 1, this model version, and the 0D version as well, closely agree with the parent SDiF model and faithfully reproduces experimental AP biomarkers. Interestingly, high value (50%) of NCX colocalization lead to unphysiological behaviors due to the presence of a large inward current in the first phases of the diastolic depolarization (Fig. 2), while concurrent low $Ca_v1.3$ (60%) and $Ca_v1.2$ ($20 - 40$%) colocalization lead to the absence of spontaneous beating.

Concerning ion channel blocks and autonomic stimulation,

Table 1. Comparison between models and experimental AP features. Cycle length (CL), Maximum Diastolic Potential (MDP), Action Potential Amplitude (APA), Overshoot (OS), Action Potential Duration at 50% repolarization (APD_{50}), Maximum Upstroke Velocity (dV/dt_{max}). Data is shown as mean ± std for the present model (values averaged on last 2s) and as mean±std (range) for experimental values.

Feature	New 3D model	New 0D model	SDiF model [4]	Experimental values [4]
$\mathbf{CL(ms)}$	292±2	330	352	325±42 (247÷389)
$\mathbf{MDP(mV)}$	-61.7±0.1	-59	-58	-56 ± 6 ($-66 \div -52$)
$\mathbf{APA(mV)}$	89±0.5	82	80	87±6 (78÷98)
$\mathbf{OS(mV)}$	27.3±0.7	23	22	27±5 (20÷32)
$\mathbf{APD_{50}(ms)}$	87.5±0.4	102	108	93±12 (73÷111)
$\mathbf{dV/dt_{max}(V/s)}$	7.9±0.1	5.4	7.1	11.3±6.5 (4.8÷27)

both models were in agreement with the original SDiF model and closely reproduced experimental data, as shown in Table 2. However, full $Ca_v1.3$ block determined cessation of pacemaking in both versions, contrarily to experimental evidence in mice showing rate decreases of -50.6% [1] and -62.5% [2]. This can be explained by the fact that with the new formulation, $I_{Cav1.3}$ has become the main current driving the action potential (see Fig. 3), and completely blocking it prevents the membrane from reaching the threshold for AP firing. Complete I_f block similarly leads to loss of automaticity and profound hyperpolarization, as in the original model. Regarding $Ca_v1.2$ channels, complete blocks results in a rate increase on both models ($+5.5\%$ and $+3.5\%$ for 0D and 3D) due to the shortening of the action potential phase.

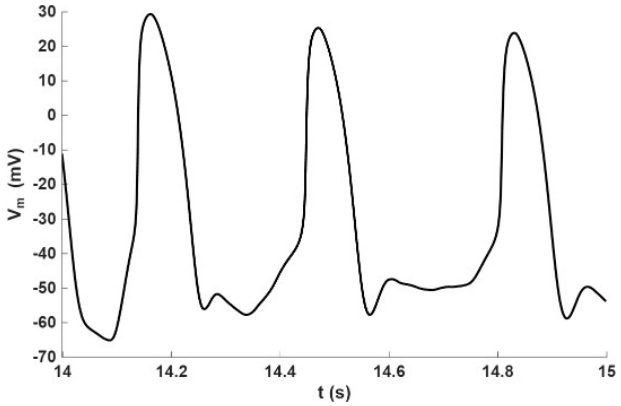

Figure 2. Action potentials of the 3D model with 50% NCX, 100% $Ca_v1.3$ and 20% $Ca_v1.2$ colocalization.

Finally, a progressive $Ca_v1.3$ block was applied to both models by reducing the maximal conductance of the channel in 10% steps. After a mild cycle length increase (up to $+13.6\%$ in 0D and $+8.6\%$ in 3D with 40% block), complete cessation of pacemaking is obtained with both model versions.

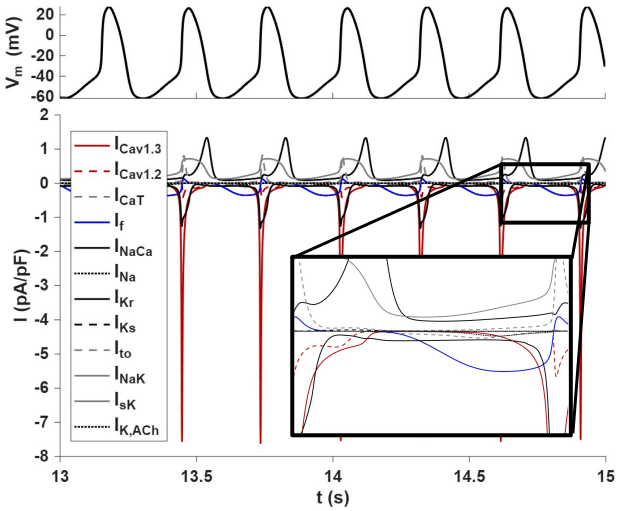

Figure 3. Action potential (top) and ionic currents (bottom) in the present 3D model. The insert highlights ionic currents in the last diastolic phase.

4. Discussion and Conclusion

In this work, we developed two different models of rabbit sinoatrial cells featuring a formulation of the $Ca_v1.3$ current from mice. The 3-dimensional model will allow the detailed investigation of pacemaking mechanisms, especially regarding Ca^{2+} fluxes and their regulation by $Ca_v1.3$ channels at the sub-cellular level. The 0D one will instead - given its lower computational cost - allow to investigate the contribution of these channels to cardiac pacemaking at the population and tissue level.

Surely, the main limitation of the present study is the use of mice data in a rabbit model. However, while species-specific data will be necessary to further develop and validate the models, interesting information can be derived from the present results. In first instance, the simulations show that the models well integrated the

Table 2. Comparison between models and experimental ion channel blocks and autonomic stimulation effects (No PM: no pacemaking activity). Percentage rate changes compared to control conditions.

Condition	New 3D model	New 0D model	SDiF model [4]	Experimental values [4]
Ctrl rate (bpm)	205	182	169	range
Iva (3 µM)	-17.7%	-22%	-22%	$-23.8 \pm 3.9\%$
100% I_f block	No PM	No PM	No PM	-
100% $Ca_v1.3$ block	No PM	No PM	-	-50.6%, -62.5% [1, 2]
100% $Ca_v1.2$ block	$+3.5\%$	$+5.5\%$	No PM	-
100% $Ca_v3.1$ block	-1.0%	-2.7%	-2.3%	-
ISO (1 µM)	$+34.6\%$	$+36.2\%$	$+28.2\%$	$+26.3 \pm 5.4\%$
ACh (10 nM)	-16.6%	-23.6%	-19.6%	$-20.8 \pm 3.2\%$

new I_{CaL} formulation, given by the sum of the $Ca_v1.3$ and $Ca_v1.2$ components. Indeed, both models showed biomarkers (in terms of action potential and responses to autonomic stimulation and ion channel blocks) in agreement with the parent model and with experimental data ranges. Interestingly, both model versions resulted to be strongly dependent on $Ca_v1.3$ current in order to show rhythmic depolarizations, given that 50% block lead to loss of spontaneous activity.

The 3D model provided additional insights on the possible ion channel arrangements in terms of colocalization with calcium release units. First of all, the "best fitting" model resulted to be the one with all $Ca_v1.3$ located in front of RyR channels but with little (20%) $Ca_v1.2$ and no NCX channels colocalized. Furthermore, high NCX colocalization values (50%) lead to unphysiologic membrane depolarizations during early diastole, hinting at low levels of exchanger channels abutting $RyRs$ or to an overestimation of LCRs contribution due to an inaccurate NCX formulation. The contribution of $Ca_v1.3$ channels might be overestimated as well, especially during the upstroke and action potential phase where these channels resulted to sustain the largest inward current. This, and the consequent loss of pacemaking at blocks higher than 50% (which is not seen in mice even with complete gene knock-out), might be explained by the species difference.

To conclude, the newly-developed rabbit SAN cell models support a key role for $Ca_v1.3$ in regulating cardiac pacemaking, making the understanding of their physiological relevance a necessity.

References

[1] Mangoni ME, Couette B, Bourinet E, Platzer J, Reimer D, Striessnig J, Nargeot J. Functional role of l-type $ca_v1.3$ ca^{2+} channels in cardiac pacemaker activity. Proc Natl Acad Sci 2003;100(9):5543–5548.

[2] Torrente AG, Mesirca P, Neco P, Rizzetto R, Dubel S, Barrere C, Sinegger-Brauns M, Striessnig J, Richard S, Nargeot J, Gomez AM, Mangoni ME. L-type cav1.3 channels regulate ryanodine receptor-dependent ca2+ release during sino-atrial node pacemaker activity. Cardiovasc Res 01 2016; 109(3):451–461. ISSN 0008-6363.

[3] Maltsev AV, Stern MD, Maltsev VA. Disorder in Ca2+ release unit locations confers robustness but cuts flexibility of heart pacemaking. J Gen Physiol 08 2022;154(9).

[4] Severi S, Fantini M, Charawi LA, DiFrancesco D. An updated computational model of rabbit sinoatrial action potential to investigate the mechanisms of heart rate modulation. J Physiol 2012;590(18):4483–4499.

[5] Mangoni ME, Traboulsie A, Leoni AL, Couette B, Marger L, Quang KL, Kupfer E, Cohen-Solal A, Vilar J, Shin HS, Escande D, Charpentier F, Nargeot J, Lory P. Bradycardia and slowing of the atrioventricular conduction in mice lacking cav3.1/α_{1g} t-type calcium channels. Circ Res 2006; 98(11):1422–1430.

[6] Mora MT, Zaza A, Trenor B. Insights from an electro-mechanical heart failure cell model: Role of serca enhancement on arrhythmogenesis and myocyte contraction. Comput Methods Programs Biomed 2023;230:107350. ISSN 0169-2607.

[7] Herrera NT, Zhang X, Ni H, Maleckar MM, Heijman J, Dobrev D, Grandi E, Morotti S. Dual effects of the small-conductance ca2+-activated k+ current on human atrial electrophysiology and ca2+-driven arrhythmogenesis: an in silico study. Am J Physiol Heart Circ Physiol 2023; 325(4):H896–H908. PMID: 37624096.

[8] Campana C, Ricci E, Bartolucci C, Severi S, Sobie EA. Coupling and heterogeneity modulate pacemaking capability in healthy and diseased two-dimensional sinoatrial node tissue models. PLOS Comput Biol 2022;18(11):e1010098.

Address for correspondence:

Eugenio Ricci

Department of Electrical, Electronic and Information Engineering, University of Bologna

Via dell'Università 50, 47522 Cesena (FC), Italy

eugenio.ricci3@unibo.it